

# Consistency, Stability and Convergence of the Viscous Garabedian and Korn (VGK) Method

Dr. Salah.J.S. El-Ibrahim\*

*Lecturer, College of Aviation Technology, P.O. Box 3357, Hawally 32034, Kuwait*

*Email: s.alhilat@collegeofaviation.com, Salah13@gmail.com*

## Abstract

The Viscous Garabedian and Korn (VGK) is a computational fluid dynamics (CFD) code, used for the prediction of viscous flows around two dimensional aerofoil sections (mapped onto a circular grid) in a subsonic free stream. The code is written in “Fortran 77” and solves the full potential flow equations using a finite difference algorithm. The code has been recently published commercially with a data preparation routine to facilitate its use [1]. The present work investigates the code’s consistency, stability and convergence in the hope that it will shed light on the code’s performance and limitations under various flow conditions and code’s numerical parameters.

**Keywords:** Artificial Viscosity; Backward Differencing Scheme; Central Differencing Scheme; Conformal Mapping; Consistency; Convergence; Grid Resolution; Numerical Oscillations; Relaxation Factor; Stability; Viscous Garabedian and Korn (VGK).

## 1. Introduction

Analytical solutions to the governing flow equations (the full Navier-Stokes equations) do not exist for the general case. Hence solutions must be obtained either experimentally or computationally. Computational fluid dynamics (CFD) involves the numerical solution of the flow equations governing fluid motion. The main uses of CFD in aeronautical applications fall under two main categories [2]. First, the provision of reliable aerodynamic predictions, enabling designers to produce “better aeroplanes”. Second, there is the possibility of using CFD for purely scientific investigations. It seems possible that numerical simulation of complex flows, not readily accessible to experimental measurements, can provide new insights into the underlying physical processes. In particular, computational methods offer a new tool for the study of turbulent structures and the mechanism of transition from laminar to turbulent flows. Cavity flows and surface irregularities may also fall under such complex flow categories, particularly in three-dimensional viscous flows.

---

\* Corresponding author.

Reflecting on the different physical behaviour of flow fields, most computational techniques and algorithms are tailored for a particular flow field [3], hence they tend to have their own (specific) applications and inherent limitations even within the intended application. Accordingly, any computational solution must be verified either experimentally or through comparison with other previously verified solutions to assess its validity and limitations. Once such criteria are established the use of the computational solution can be justified. Experimental work, therefore, -although time consuming and expensive on resources- is still a necessity, particularly if no other previously validated solution exists to compare with the one under investigation. In addition to the validation/verification process, the computational solution must also be assessed for the reliability and quality of its numerical solution. This can be done by analysing the Stability, Consistency, and Convergence of the algorithm(s) used in the numerical calculations. The present work attempts to investigate these aspects (Stability, Consistency and Convergence) of the VGK method and to describe the factors affecting its solutions under various flow conditions.

## 2. The VGK Method

The Viscous Garabedian and Korn (VGK) is a computational fluid dynamics (CFD) code, used for the prediction of viscous flows around two dimensional aerofoil sections (mapped onto a circular grid) in a subsonic free stream. The code is written in “Fortran 77” and solves the full potential flow equations using a finite difference algorithm. The code was published commercially with a data preparation routine to facilitate its use [1]. Because of its relative simplicity in use and computational economy, VGK offers a convenient method for the assessment of the effects of small deviations from a specified aerofoil profile, such as may be caused by damage or manufacturing errors [4]. The reliable assessment of such imperfections enables a decision to be made as to whether to tolerate, repair, or reject the surface under investigation. In the aircraft industry the decision involves three important considerations: flight safety, money and time. However, to reach a decision the assessment process itself may be both costly and lengthy and in the end may not be fully reliable. This highlights the importance of relying on a code that will provide quick and reliable answers to the decision maker. VGK offers simplicity of use and had been proved [5] to provide valid solutions to high speed subsonic flows (up to the point where weak shock waves may exist) around aerofoils with surface imperfections provided that these imperfections do not sharply change the curvature of the profile, also under flow conditions where weak shock waves can present in the flow. Therefore, for a simple and direct assessment method it is hoped that VGK will provide quick and reliable answers.

### 2.1 VGK Capabilities and Limitations

The Viscous Garabedian and Korn (VGK) code is a computational fluid dynamics code written in Fortran 77, and based on the coupled solution of the inviscid and viscous flow regions of two-dimensional transonic attached flow past an aerofoil in a subsonic free stream. The full potential equations governing the inviscid flow region, formulated on the assumptions of steady and compressible flow of air (with specific heats ratio  $\gamma = 1.4$ ), are solved by a finite difference technique. The viscous flow region is solved using the integral equations governing the laminar and turbulent boundary layer components, and solutions involve the displacement and momentum thickness distributions of the boundary layer and wake, which are calculated allowing for the effects of the pressure distribution obtained from the inviscid flow solution. The boundary conditions for the inviscid

flow solution specify a non-zero normal velocity at the aerofoil surface to allow for the growth of the boundary layer displacement surface, and a jump in velocity across the dividing streamline to allow for the wake thickness and curvature effects. This introduces the concept of “Equivalent Inviscid Flow-EIF”. This means that the “actual inviscid” flow region is replaced by an “equivalent inviscid flow region, that, by definition, extends right onto the wall (the aerofoil surface), and a convenient line in the wake dividing the flow of the upper and lower surfaces of the aerofoil. VGK employs a central-difference and a backward difference schemes (for fully subsonic and supersonic flow regions respectively) of the Taylor series expansion of the full potential flow equation (equation (1) below). VGK uses computational grid in the solution which is an O-type grid. It is generated by conformally mapping the infinite region outside the aerofoil into the inside of a unit circle. The grid points are defined by the intersection of radial lines emanating from the aerofoil surface and concentric circles circumferentially placed around the aerofoil, so the grid is allowed to touch the aerofoil surface. The computational grid is calculated by the VGK code utilising the aerofoil surface co-ordinates. VGK requires that for the grid to be satisfactory, it is necessary (but not sufficient) that the input aerofoil co-ordinates must be closely pitched, specially near the leading and trailing edges, and also be sufficiently smooth to yield smooth first and second order derivatives. VGK employs an iterative scheme to calculate the computational grid using a spline interpolation of the input aerofoil co-ordinates for each iteration step, and with about 30 iteration steps convergence is rapid for most of the aerofoil geometries of interest. Grid sequencing is employed in VGK to reduce the truncation error (residuals) at all the grid nodes and only two grids are used in VGK for this purpose: a coarse grid constituting 80 radial lines x 15 circumferential circles, and a fine grid that constitutes 160 lines x 30 circles. The VGK solution process starts with the evaluation of the computational grid. Once this is achieved, the iteration solution of the finite difference equations for the inviscid flow potential proceeds by a relaxation method in which the values of potential obtained at the end of each iteration step are multiplied by a factor (called a relaxation factor). When this factor is greater than unity the process is termed over relaxation and when under unity the term under-relaxation is used. The associated factors are called over relaxation or under-relaxation factors respectively. Over- or under-relaxation is used to increase the rate of convergence or avoid divergence depending on the form of the finite difference equations. In VGK different relaxation factors are used for the finite difference equations corresponding to subsonic and supersonic flow regions and the default values of these factors are set at 1.9 and 1.0 respectively. A relaxation process is also used in introducing the boundary conditions corresponding to the viscous flow element into the inviscid flow. A number of inviscid flow iterations (typically 5) are carried out between each occasion the boundary conditions are updated, and the calculated changes to these boundary conditions are decreased by an under-relaxation factor (typically 0.15 for the fine grid and 0.075 for the coarse grid). The final coupled (viscous-inviscid) solution is considered to be converged when the fine grid residuals in both the viscous and inviscid equations have reduced to a level beyond which any changes, as a result of further iterations, will have zero or negligible effects on the calculated flow parameters. In addition to the basic pressure distribution over the aerofoil surface, VGK provides a number of local surface parameters, such as Mach number (M), pressure ratio (local static pressure/stagnation), and pressure coefficient, and overall parameters such as lift, drag and pitching moment coefficients. Data related to boundary layers and wake are also output, these include: shape parameter, displacement and momentum thicknesses, skin friction coefficient and boundary layer thickness for the upper and lower surfaces boundary layer, and pressure coefficient, pressure ratio, and Mach number for the lower and upper parts of the wake.

Certain “numerical control parameters” are used in VGK to control the grid density, rate of convergence and the form of the finite difference scheme employed in any supersonic flow region. These parameters influence the results obtained by any VGK run, hence they must be carefully chosen to generate the most reliable data. However, VGK uses default values for these parameters (known as “default parameters”) which are generally suited for most flow conditions provided no strong shock waves or separated boundary layers are present. For flows with moderate shock waves or boundary layer being close to separation these parameters may be changed to enable convergence and “reliable” data to be obtained. Table (1) gives a summary of these parameters and their related influence on the calculated flow. The VGK code has some limitations; for example, there is no method in VGK for predicting boundary layer transition location, & the user has to input the location for the upper and lower surfaces. If the calculated local skin friction coefficient becomes less than a limiting value ( $=2 \times 10^{-6}$ ) separation of the laminar boundary layer is assumed to occur at this location and the transition point is moved to this location instead of the specified one. This may be thought of as a simplified model for a short bubble laminar separation/ turbulent re-attachment which would normally occur in practice [6]. There is also no check applied within VGK that the boundary layer could actually become turbulent at the specified transition points and remain turbulent thereafter. Solutions in VGK will not converge for difficult flow conditions associated with strong shock waves ( $M_{shock} > 1.4$ ) or regions of extensive boundary layer separation.

**Table 1:** VGK Numerical parameters

PARAMETER & DEFINITION	VALUE			EFFECTS OF CHANGES ON THE FLOW
	DEFAULT	MAX.	MIN.	
a). NSG, Number of the radial mesh lines in the fine grid*	160	160	96	Very slight effects for flows without shocks, Lower values give less steep shock pressure rises, and milder effects on the boundary layer
b). NSC, Number of iterations of the inviscid flow element using the coarse mesh	100	May be double d (see f below)	0	Default value generally adequate to reduce the level of residuals for the commencing fine grid convergence
c). NSF, Number of iterations of the inviscid flow elements using the fine mesh	200	May be double d (see f below)	----	Default value generally provides adequate convergence level; a further few hundred iterations may be needed if the residuals are declining, or if the $C_L$ value has not stabilised after 200 iterations
d).XS, The subsonic flow relaxation parameter	1.9	<2	>0	For difficult flows lower values may be needed to avoid divergence, values down to 1.6 may confer advantages
e).XM, The supersonic flow relaxation parameter	1	1	>0	Same as XS above, lower values down to 0.8 may confer advantages
f).EP( $\varepsilon$ ),Artificial viscosity parameter**, and QCP( $\lambda$ ),Partially-conservative parameter***	$\varepsilon = 0.8$ $\lambda = 0.25$			These two parameters jointly influence the computed supersonic flow.

NOTES on table (1):

\* There is no facility in VGK for changing the number of circumferential lines in the fine grid.

\*\* The artificial viscosity parameter is  $\varepsilon$  is added into the finite differencing equations to allow for the inclusion of higher order terms and reduce the discretisation error.

\*\*\* The partially conservative parameter  $\lambda$  is a shock point operator [13], it is assigned any value between 0.0 and 1.0 and is meant to simulate conservative ( $\lambda = 1$ ) or non-conservative schemes ( $\lambda = 0$ ). Thus improving the pressure jump through a shock wave.

However, for flows with moderate difficulties ( $1.2 < M_{shock} < 1.4$ ), convergence may be achieved in steps, that is to arrive at the run under question as a continuation run to previous runs achieved with lower Mach number, lower incidence or higher Reynolds' number. It has also been found that VGK solutions can exhibit numerical oscillations when large changes in profile curvature are encountered (aerofoils with indentations). The present work attempts to investigate the numerical behaviour of VGK under various flow conditions for the purposes of assessing its overall reliability and identifying the factors (in the numerical schemes) that may cause calculations issues in the hope of finding ways to improve the code's performance.

## 2.2 Limitations/Constraints of the present work

For brevity, the present work is limited to the theoretical analysis of the numerical behaviour of the VGK code solution to the 2-D potential flow partial differential equations. VGK runs with changing numerical parameters (table 1 above) and flow conditions to simulate difficult flow conditions were not performed here as these will have to cover various free stream conditions (different free stream Mach numbers,  $M_\infty$ , and angles of attack), and in the present author's opinion these are to be left to a separate future work.

## 3. Definitions

In any numerical scheme three main features must be addressed in order to provide sound judgement on the behaviour of the scheme in terms of the overall accuracy and representation of the original or discretized partial differential equation. These features are the concepts of consistency, stability and convergence of the scheme [7], which are briefly defined as follows:

### 3.1 Consistency

A requirement that imposes a condition on the structure of the numerical formulation (discretized equation) and how well it represents the original partial differential equation. This provides an insight into the order of the discretization error. This is analysed by writing out the Taylor series expansion of the discretized elements and comparing the result to the original partial differential equation. The discretization error will then be the difference between the two and the consistency requirement states that "*The discretization error will tend to zero when the mesh spacing in the discretization direction (or a time step) tends to zero*" [7].

### 3.2 Stability

This condition establishes the relationship between the numerical and exact solutions of the discretized equation. Within the stability requirements it is emphasized that this difference (error) should diminish (or be bound) for  $n \rightarrow \infty$ , where  $n$  represents the total number of iterations (or time steps).

### 3.3 Convergence

This represents the relationship between the numerical solution and the exact solution of the differential equation. The difference between these two solutions is known as the solution error and the convergence condition establishes that this error should reduce to zero as the grid is refined. It is usually very difficult to establish the convergence criterion theoretically particularly for flow cases where the exact solution is not known. The convergence of a finite difference scheme is related to the stability and consistency by the Lax equivalence theorem [9], which states that: “*Given a well-posed linear initial value problem and a finite difference approximation to it that is consistent, stability is the necessary and sufficient condition for convergence*” The Lax equivalence theorem is of great importance since it is relatively easy to show the stability of an algorithm and its consistency with the original differential equation. However as most real flow problems are non-linear and are boundary or mixed initial/boundary value problems the Lax theorem cannot always be applied hence it should be interpreted as providing the necessary but not always sufficient condition for convergence.

## 4. Investigating the Consistency, Stability & Convergence of the VGK Scheme

The investigations here are based on analysing the central and backward difference schemes of the Taylor series expansions of the full potential flow equation applied to the circular grid points (i, j).

The potential flow equation used in VGK is given by (see definitions of mathematical symbols):

$$(a^2 - \bar{u}^2)\Phi_{\theta\theta} - 2r\bar{u}\bar{v}\Phi_{r\theta} + r^2(a^2 - \bar{v}^2)\Phi_{rr} - 2\bar{u}\bar{v}\Phi_\theta + r(a^2 + \bar{u}^2 - 2\bar{v}^2)\Phi_r + r^{-1}(\bar{u}^2 + \bar{v}^2)(\bar{u}f_\theta + r\bar{v}f_r) = 0 \quad (1)$$

Where:  $a$  is the local speed of sound,  $\bar{u}, \bar{v}$  the tangential and normal velocities components respectively in the computational plane,  $r, \theta$  the grid radial and angular coordinates,  $\Phi$  the velocity potential in the computational plane. (With subscripts indicating first, second and mixed derivatives with respect to  $(r, \theta)$ ,  $f$  the modulus of the mapping function with subscripts in  $(r, \theta)$  representing derivatives of  $f$  with respect to  $(r, \theta)$ ) The code solves for the flow potential ( $\Phi$ ) using central differencing scheme for the subsonic flow regions and forward/backward differencing scheme for the supersonic flow regions [10]. Central differencing, applied throughout the subsonic region along the tangential and radial lines:

$$\Phi_\theta = \frac{\Phi_{i+1,j} - \Phi_{i-1,j}}{2\Delta\theta}$$

$$\Phi_r = \frac{\Phi_{i,j+1} - \Phi_{i,j-1}}{2\Delta r}$$

$$\Phi_{rr} = \frac{\Phi_{i,j+1} - 2\Phi_{i,j} + \Phi_{i,j-1}}{(\Delta r)^2}$$

$$\Phi_{\theta\theta} = \frac{\Phi_{i+1,j} - 2\Phi_{i,j} + \Phi_{i,j-1}}{(\Delta\theta)^2}$$

$$\Phi_{\theta r} = \frac{\Phi_{i+1,j+1} - \Phi_{i-1,j+1} + \Phi_{i-1,j-1} - \Phi_{i+1,j-1}}{4\Delta r\Delta\theta}$$

Where the (i, j) subscripts representing the  $i^{\text{th}}$  and  $j^{\text{th}}$  steps and  $\Delta r, \Delta\theta, \delta r, \delta\theta$  are the step sizes in the  $r, \theta$  directions respectively in the computational plane:

In the supersonic (hyperbolic) region backward differences are used on the upper surface ( $\pi \leq \theta \leq 2\pi$ ) and forward differences on the lower surface ( $0 \leq \theta \leq \pi$ ) in the following manner:

$$(\Delta\theta)^2 \Phi_{\theta\theta} = (\Phi_{i,j} - 2\Phi_{i\mp1,j} + \Phi_{i\mp2,j}) + \varepsilon(\Phi_{i,j} - 3\Phi_{i\mp1,j} + 3\Phi_{i\mp2,j} - \Phi_{i\mp3,j})$$

and

$$4\Delta\theta\Delta r \Phi_{\theta r} = 2(\Phi_{i,j\pm1} - \Phi_{i\mp1,j\pm1} + \Phi_{i\mp1,j\mp1} - \Phi_{i,j\mp1}) + \varepsilon(\Phi_{i,j\pm1} - 2\Phi_{i\mp1,j\pm1} + \Phi_{i\mp2,j\pm1} - \Phi_{i\mp2,j\mp1} + 2\Phi_{i\mp1,j\mp1} - \Phi_{i,j\mp1})$$

where for the indices  $(i, j)$ , the upper sign is used for the backward difference scheme and the lower sign for the forward scheme.

The governing equation (1) is of the form:

$$A\Phi_{\theta\theta} + B\Phi_{r\theta} + C\Phi_{rr} = D \quad (2)$$

where:

$$\begin{aligned} A &= (a^2 - \bar{u}^2), & B &= -2\bar{u} \bar{v} r, & C &= r^2(a^2 - \bar{v}^2) \\ D &= 2\bar{u}\bar{v}\Phi_\theta - r(a^2 + \bar{u}^2 - \bar{v}^2)\Phi_r - r^{-1}(\bar{u}^2 + \bar{v}^2)(\bar{u}f_\theta + \bar{v}f_r r) \end{aligned} \quad (3)$$

and applies outside the viscous layers. To solve for  $\Phi$  a finite difference representation of (2) is formed by a tri-diagonal system of equations:

$$a_{ij}\Phi_{i,j-1} + b_{ij}\Phi_{i,j} + c_{ij}\Phi_{i,j+1} = d_{ij} \quad (4)$$

Here  $a_{i,j}, b_{i,j}, c_{i,j}, d_{i,j}$  are the coefficients of the potential equation the finite difference form.

#### 4.1 Analysing the Consistency of VGK

it can be shown that for the centre-differencing scheme, the total truncation error is given by:

$$(\text{Error})_{\text{total}} = -\frac{A}{12}(\Delta\theta)^2\Phi_{\theta\theta\theta} - \frac{C}{12}(\Delta r)^2\Phi_{rrr} - \frac{B}{6}(\Delta\theta)^2\Phi_{r\theta\theta\theta} \quad (5)$$

Equation (5) is second order in  $(\Delta r, \Delta\theta)$ , and shows that the central difference scheme is consistent. This, also, gives the coefficients of the fourth derivatives of  $\Phi$  in  $\theta$  and  $r$  (or the third derivatives of the velocities  $\Phi_\theta$  and  $\Phi_r$ ) i.e. an odd-order derivative as the dominant term in the truncation error. This represents a diffusive term (dispersive) implicitly imbedded in the central difference scheme [7]. The exact amount and sign (whether lagging or leading) of this dispersion will, of course, be dependent on the actual values of the coefficients  $A$ ,  $B$ , and  $C$  at every point in the grid. It is, however, difficult to assess analytically the value of (5) but it will not be of major concern here as it will be very small and tending to zero as both  $\Delta\theta$  and  $\Delta r \rightarrow 0$ .

In the backward difference scheme, the truncation error takes the following forms:

$$(\text{Error})_{\text{total}} = A(\Delta\theta)(1-\varepsilon)\Phi_{\theta\theta\theta} + \frac{B}{2}(\Delta\theta)(1-\varepsilon)\Phi_{\theta\theta r} - \frac{C}{12}(\Delta r)^2\Phi_{rrr} \quad (6)$$

with  $0 \leq \varepsilon = 1 - \lambda(\Delta\theta) \leq 1$ , equation (6) becomes:

$$(\text{Error})_{\text{total}} = \lambda(\Delta\theta)^2 \left[ A\Phi_{\theta\theta\theta} + \frac{B}{2}\Phi_{\theta\theta r} \right] - \frac{C}{12}(\Delta r)^2\Phi_{rrr} \quad (7)$$

With  $(\varepsilon)$  being an artificial viscosity parameter. When  $(\varepsilon = 0)$  equation (6) is first order accurate in  $(\Delta\theta)$  but second order in  $(\Delta r)$ , however with the addition of  $(\varepsilon)$  this becomes second order accurate in both  $(\Delta\theta \& \Delta r)$  as shown in (7). Equation (7) represents the coefficients of the second derivatives of the velocities  $\Phi_\theta$  &  $\Phi_r$  and thus an artificial viscosity term (dissipative) that is either implicitly present in the original scheme (i.e. when  $\varepsilon = 0$ ) or explicitly modified by the introduction of the parameter  $\varepsilon$ . The introduction of this parameter reduces the value of the implicit dissipation by a factor of  $\lambda\Delta\theta$  (or by  $(1-\varepsilon)$ ) so that not too much dissipation is introduced in the original scheme. It is therefore immediately concluded that reducing  $\Delta\theta$  (by increasing the number of mesh radial lines) in the hope of increasing the accuracy, may in fact cause an oscillatory behaviour (because of the reduced dissipation). A qualitative assessment of this can be arrived at by explicitly writing the coefficients  $A$  and  $B$  in (7) using equation (3), hence (7) becomes:

$$(\text{Error})_{\text{total}} = \lambda(\Delta\theta)^2 [(a^2 - \bar{u}^2)\Phi_{\theta\theta\theta} - (\bar{u}\bar{v}r)\Phi_{\theta\theta r}] \quad (8)$$

In hyperbolic regions, for which this equation holds, and if flow conditions are leading to the formation of a shock wave, it is expected that  $\bar{u}$  will be of the same order as  $a$ . Hence the coefficient of  $\Phi_{\theta\theta\theta}$  will be very small making (8) tend to a negative value unless  $\Phi_{\theta\theta r}$  is negative (maximum  $\Phi_r$ ). With the presence of a small factor  $\lambda(\Delta\theta)^2$  and these conditions, the dissipation term is reduced and oscillatory behaviour may ensue.

Two other important aspects of the dissipation behaviour can be revealed through (8):

- As  $\Phi_\theta$  and  $\Phi_r$  increase towards their maximum values then it is expected that their second derivatives ( $\Phi_{\theta\theta\theta}$  and  $\Phi_{\theta\theta r}$ ) will become negative. This will help make (8) positive thus aiding a stable behaviour of the scheme when  $\bar{u} > a$ . This situation happens when the flow is completely supersonic, for example upstream of a shock wave.
- The velocity components in the computational plane ( $\bar{u}$  and  $\bar{v}$ ) are related to the potential velocities ( $\Phi_\theta$  and  $\Phi_r$ ) and the mapping modulus ( $f$ ) by:

$$\bar{u} = \frac{f}{r} \frac{\partial \varphi}{\partial \theta}, \quad \bar{v} = f \frac{\partial \varphi}{\partial r}$$

Substituting these into (8) gives:

$$(\text{Error})_{\text{total}} = \lambda(\Delta\theta)^2 [(a^2 - f^{-2}r^2\phi_\theta^2)\Phi_{\theta\theta\theta} - (f^{-2}r^4\phi_\theta\phi_r)\Phi_{\theta\theta r}] \quad (9)$$

It is apparent that for small values of  $f$  equation (9) may become negative, this is most likely the case when  $(\Phi_{\theta\theta\theta})$  is positive corresponding to a reducing tangential velocity; that is after passing the maximum suction point on the upper surface. This is related to the aerofoil geometry since  $f = \frac{ds}{d\theta}$ . It is thus to be expected that aerofoils with a sharp change in profile, (a sudden or a sharp decrease in the first derivative) occurring after the maximum suction point may exhibit an oscillatory behaviour particularly at reducing speeds (e.g. downstream of a shock wave). In summary, the above merely states that in a hyperbolic region dissipation is reduced as  $\Delta\theta \rightarrow 0$ , and oscillatory behaviour will be promoted by a sharp reduction (or a sudden change) in profile first derivative after the maximum suction point and in the presence of pressure gradient downstream of a shock wave. Figure (1) below shows the variation of the dissipation factor  $\lambda(\Delta\theta)^2$  with the artificial viscosity parameter  $\varepsilon$  at various values of  $\Delta\theta$  where it is shown that to keep a satisfactory level of dissipation at a reduced  $\Delta\theta$  the value of  $\varepsilon$  must also be reduced.

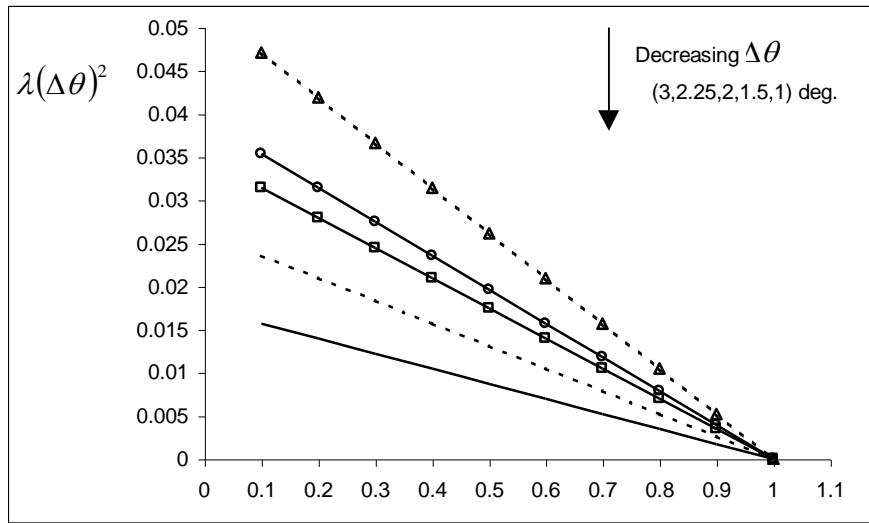


**Figure 1:** Dissipation factor variation with artificial viscosity at different values of  $\Delta\theta$

#### 4.2 Analysis of the Stability of the VGK

The Von Neumann method [7,8] for stability analysis was used to check the stability of the VGK method. The analysis for the central and backward difference schemes reveals that the central difference scheme is unconditionally stable, thus any oscillatory behaviour at totally subsonic speeds (non-existing supersonic regions) will be geometry-related, and caused by the application of the cubic spline in the conformal mapping procedure to regions of highly varying curvature.

For the hyperbolic regions the stability criterion is given by the following formula:

$$K_1(a^2 - u^2)^2 - K_2(a^2 - v^2)^2 + K_3(uv)^2 + K_4(a^2 - u^2)(a^2 - v^2) \leq 0.0 \quad (10)$$

where  $(u, v)$  are the local stream-wise and normal velocity components in the physical plane, and  $K_1$  to  $K_4$  are positive constants that depend on the mesh spacing ( $\Delta\theta$  &  $\Delta r$ ) and the artificial viscosity parameter  $\varepsilon$ , defined by the following:

$$K_1 = 4 \left( \frac{1 + 4\varepsilon + 4\varepsilon^2}{(\Delta\theta)^4} \right), \quad K_2 = \left( \frac{2}{(\Delta r)^4} \right), \quad K_3 = \frac{1}{8} \left( \frac{2 + \varepsilon}{(\Delta\theta)(\Delta r)} \right)^2, \quad K_4 = 4 \left( \frac{1 + \varepsilon}{(\Delta\theta)^2(\Delta r)^2} \right)$$

Figures (2,3) show the variations of  $K_1$  to  $K_4$  with the total number of mesh radial lines for  $\varepsilon = 0.0$  and  $\varepsilon = 1.0$  respectively, (in VGK  $\Delta r$  is fixed at  $\frac{1}{30}$ ). These show that for  $\varepsilon = 0$ ,  $K_1$  dominates the other coefficients for  $m \geq 220$  where  $m$  is the total number of grid radial lines. This corresponds to  $\Delta\theta \leq 0.03\text{rad}$  approximately. On the other hand for  $\varepsilon = 1$ ,  $K_1$  starts to dominate the other coefficients for

$m \geq 160$ , that is  $\Delta\theta \leq 0.039\text{rad}$ . With  $(\varepsilon = 0)$  this domination is also more apparent when the coefficients  $K_1$  to  $K_4$  are normalized by  $K_1$  as shown in figure (4). Here the region of domination of  $(K_1)$  is shown (inset of figure 4).

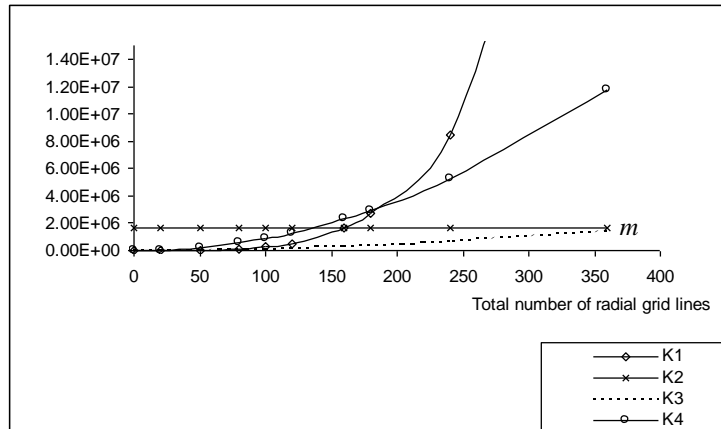


**Figure 2:** Variations of the stability equation coefficients with number of grid lines at  $\varepsilon = 0$

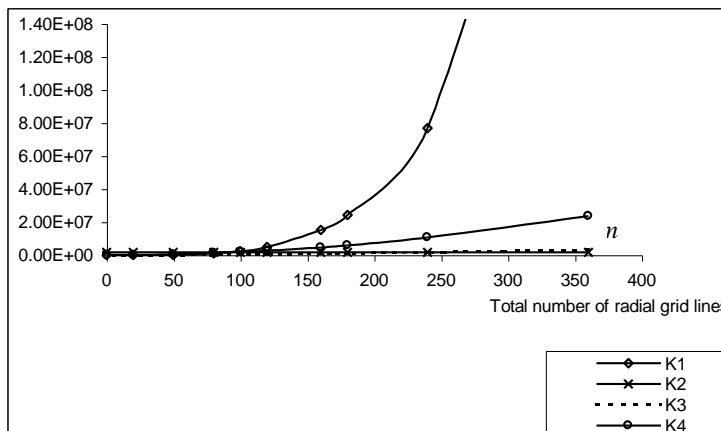


**Figure 3:** Variations of the stability equation coefficients with number of grid lines at  $\varepsilon = 1$

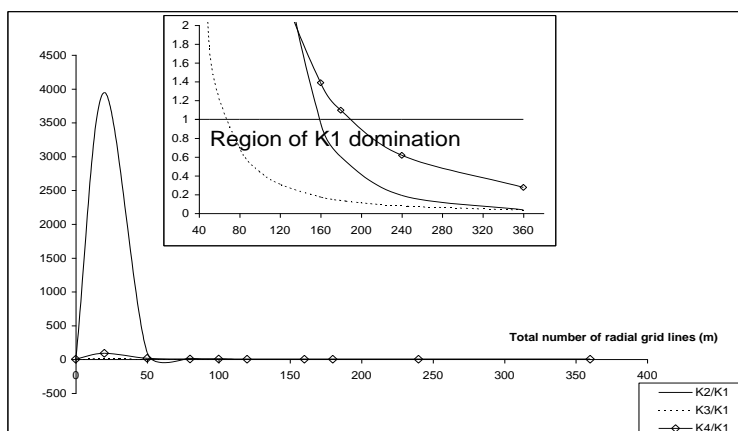


**Figure 4:** Stability equation coefficients normalized by  $K_1$  ( $\varepsilon = 0$ )

Examining figures (2-4) in conjunction with equation (16) reveals that when:

- $u > a$

The term associated with  $K_4$  is negative, and together with the  $K_2$  term dominate the  $K_1$  term when  $80 \leq m \leq 180$  approximately, so in this case equation (16) is satisfied and the stability of the scheme is ensured. For  $m \leq 80$  the  $K_3$  term dominates the other terms and unless this is offset by the value of  $uv$ , instabilities may occur.

- $u O[a]$  and  $< a$

Domination of the  $K_2$  term over the  $K_3$  term will govern the stability condition, this is the case for  $m \leq 220$  approximately, (see inset of figure 7.8), unless  $uv \gg (a^2 - v^2)$ . The above only forms a general guideline on the effects of the local flow conditions (when coupled with  $m$ ) on the overall stability behaviour of the hyperbolic scheme. The actual behaviour will of course depend on the particular values in equation (10).

#### **4.3 Analysing the Convergence of the VGK method**

The consistency and stability are necessary but not sufficient conditions for convergence. However, since VGK solves a tri-diagonal system (formed by equation 4), to satisfy convergence the diagonal dominance of the coefficient matrix in (4) must also be ensured [11]. The diagonal dominance of a matrix is ensured if the following condition is satisfied:

$$|a_i| + |c_i| < |b_i| \quad (11)$$

where  $a_i, b_i$  and  $c_i$  constitute the row elements of the tri-diagonal coefficient matrix. It can be shown that the values for  $a_i, b_i$  and  $c_i$  in terms of the coefficients  $A, B, C$ , and  $D$  of the difference equation (2) can be written as:

- For the central difference (subsonic region)

$$a_{i,j} = C\delta^2$$

$$b_{i,j} = -2[A + C\delta^2]$$

$$c_{i,j} = C\delta^2$$

- For the backward Difference (Supersonic region):

$$a_{i,j} = \left[ \delta^2 C - \frac{(2+\varepsilon)}{4} \delta B \right]$$

$$b_{i,j} = [-2\delta^2 C + (1+\varepsilon)A]$$

$$c_{i,j} = \left[ \delta^2 C + \frac{(2+\varepsilon)}{4} \delta B \right]$$

where  $A = a^2 - \bar{u}^2$ ,  $B = -2\bar{u}\bar{v}r$ ,  $C = a^2 - \bar{v}^2$  and  $\delta = \frac{\Delta\theta}{\Delta r}$ .

Applying these to the dominance equation (11) the following conditions are arrived at:

- For the central difference (subsonic) scheme

$$2A^2 + 4\delta^2 AC + C^2 \delta^4 > 0.0 \quad (12)$$

- For the backward difference (supersonic) scheme

$$A(1+\varepsilon) - 4C\delta^2 + 2\frac{\delta^4}{A(1+\varepsilon)} C^2 > \frac{1}{2} \delta^2 \frac{(2+\varepsilon)^2}{A(1+\varepsilon)} B^2 \quad (13)$$

Equations (12 and 13) apply to all internal mesh points, but exclude the unit circle representing the boundary where in the tri-diagonal matrix the boundary is represented by the elements of the first row ( $j = 1$ ). The central difference scheme (equation 12) shows unconditional diagonal dominance and since in this flow regime the scheme was shown to be unconditionally stable it is immediately concluded that convergence is assured provided no geometry-related instabilities take place. In the hyperbolic regions, however, equation (13) places certain restrictions on the mesh spacing  $\Delta\theta$  and  $\Delta r$ , the local speed conditions  $(\bar{u}, \bar{v})$  and the amount of artificial viscosity  $\varepsilon$ . Accordingly it is difficult to assess the conditions for which diagonal dominance can be ensured in these regions of the flow except to state that it appears from equation (19) that for all  $\delta > 1$  (that is

$\Delta\theta > \Delta r = \frac{1}{30}$ , or  $m \leq 188$  approx.), increasing  $\delta$  (reducing  $m$ ) helps convergence. Also since

$B = -2\bar{u}\bar{v}r$  and  $r$  decreases away from the boundary towards the centre of the mesh (i.e. towards physical infinity), then it can also be deduced from (13) that, given the same flow conditions diagonal dominance is more attainable away from the boundary. On the boundary ( $r = 1$ ) the coefficients in equations (12 and 13) take the following forms (see appendix B of reference 12).

- Central difference (subsonic) scheme:

$$a_{i,1} = 0$$

$$b_{i,1} = -2(A_1 + \delta^2 C_1) \quad (14)$$

$$c_{i,1} = 2\delta^2 C_1$$

- Backward difference (supersonic) scheme:

$$a_{i,1} = 0$$

$$b_{i,1} = (1 + \varepsilon)A_1 - 2\delta^2 C_1 \quad (15)$$

$$c_{i,1} = 2\delta^2 C_1$$

where the subscript 1 indicates conditions on the boundary. In the central difference scheme, diagonal dominance of the first row of the coefficient matrix is then given by:

$$A_1^2 + \delta^2 A_1 C_1 > 0$$

which again gives unconditional diagonal dominance.

In the backward difference scheme the equivalent condition is:

$$(1 + \varepsilon)A_1 [(1 + \varepsilon)A_1 - 4\delta^2 C_1] > 0$$

this gives

$$\delta^2 < \pm \frac{(1 + \varepsilon)A_1}{4C_1} \quad (16)$$

where the upper sign refers to positive  $A_1$  (that is  $u < a$ , but with  $u^2 + v^2 > a^2$  to stay supersonic) and the lower sign refers to negative  $A_1$ . This shows that the favourable increase in  $\delta$  for convergence as stipulated by equation (13) must be restricted by an upper limit given by equation (16). This analysis depends on an assumed prior knowledge of  $A_1$  and  $C_1$ , which is difficult since these form part of the solution. Nevertheless, for each row of the diagonal matrix representing a new circle in the mesh an iterative procedure is used whereby each iteration cycle moves along the present circle calculating the potential values at each radial point. For each circle a number of iterations is carried out for the coarse and fine grids (default values are 100 and 200 respectively). A relaxation process is used to speed up and help convergence. This relaxation process is given by the following formula:

$$\Phi_{i,j}^{K+1} = xR_{i,j} + (1-x)\Phi_{i,j}^K$$

where  $K$  is an iteration number,  $R_{i,j}$  is the initial calculated value of the potential obtained by solving the tri-diagonal system at the point  $(i, j)$  and consequently forms the value of  $\Phi_{i,j}$  from the previous iteration. The relaxation factor ( $x$ ) is defined by:

$$x = \text{Min}\{x_s, \text{Max}\{x_m, P\}\} \quad (17)$$

where, again,  $x_s$  is an over-relaxation factor specified by the user, ( $1 \leq x_s \leq 2$ , default value=1.9),  $x_m$  is an under-relaxation factor also specified by the user ( $0 \leq x_m \leq 1$ , default value=1), and  $P$  a variable which depends on local and free stream conditions and is defined by:

$$P = x_s - \left( \frac{x_s - x_m}{1 - q_{crit}^2} \right) (1 - q^2) \quad (18)$$

with  $q$  and  $q_{crit}$  being the total local and critical speeds respectively and  $q$  is given by:

$$q^2 = u^2 + v^2 = a^2.$$

Thus the relaxation parameter is constant ( $x_s$  or  $x_m$ ) unless  $P$  is used. Equation (17) determines the condition for which the use of  $P$  is invoked, and that is when:

$$x_m < P < x_s$$

substituting for  $P$  from (18) gives:

$$x_m < x_s - \left( \frac{x_s - x_m}{1 - q_{crit}^2} \right) (1 - q^2) < x_s$$

that is

$$1 > \left( \frac{1 - q^2}{1 - q_{crit}^2} \right) > 0$$

or finally the relaxation factor  $x = P$  is used when

$$q_{crit}^2 < q^2 < 1 \quad (19)$$

which indicates that in the supersonic range given by (19) a variable relaxation factor is used and is dependent on the local speed conditions. The shaded area in figure (5) shows this.

To investigate the effects of  $P$  it can be written from (18) as:

$$P = L_1 q^2 + L_2$$

where from (18)  $L_1, L_2$  are constants and are given by:

$$L_1 = \frac{x_s - x_m}{1 - q_{crit}^2} , \quad L_2 = \frac{x_m - x_s q_{crit}^2}{1 - q_{crit}^2}$$

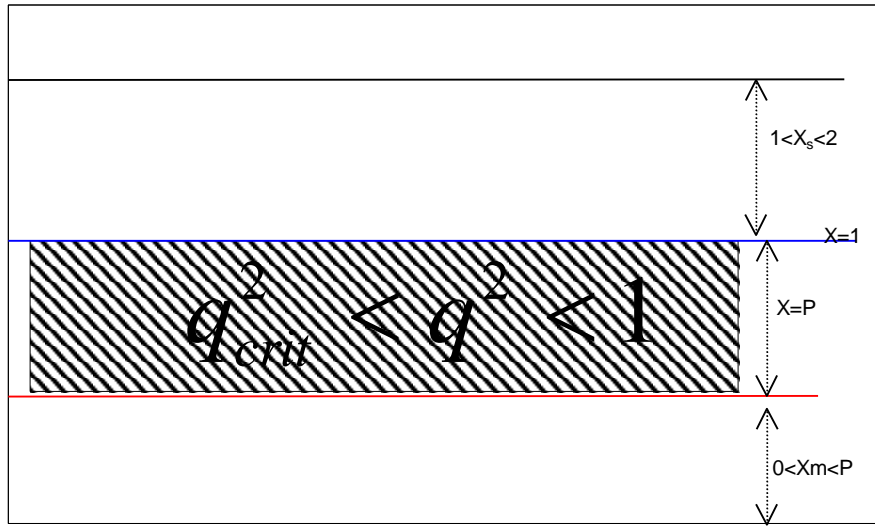


**Figure 5:** Region where a variable relaxation factor P is used (shaded)

Since  $q$  represents the gradient of the potential,  $\Phi$ , and forms part of the iterative solution, any oscillations imply that  $q$  itself will be oscillatory. This oscillatory behaviour may be further amplified through  $P$  via the  $L_1 q^2$  term, leading to an unstable (diverging) solution. To help convergence in such regions it would seem preferable to set  $x_m = 1$  so that  $P$  is never used, thus it is hoped, that a final non-oscillatory solution will be reached through increasing the number of iterations, if necessary. A final word of warning regarding convergence in VGK should be introduced here. Iterations proceed either if the total number of iterations is below a pre-specified number or the tolerance is exceeded, whichever occurs first. If the specified maximum number of iterations is reached then VGK outputs the various flow parameters (surface and wake pressures, velocities...etc.) even if the tolerance is exceeded. Though these may not represent a final converged (or accurate) solution. To investigate the accuracy of the solution the convergence history against the number of iterations (which can be increased successively for a number of runs) must be checked. This can be done by inspecting the residuals (output in the file with extension “.IEH”) for each of the successive runs. The most reliable solution will then be the one after which any increase in the number of iterations does not produce a significant change in the residuals.

## 5. Results and Conclusions

The preceding analysis showed that the numerical calculations performed by the Viscous Garabedian & Korn (VGK) code are:

A. Consistency:

I. The central differencing scheme is unconditionally stable. (the truncation error is second order accurate

in  $(\Delta\theta)$  and  $(\Delta r)$

- II. The backward differencing scheme is first order accurate in  $(\Delta\theta)$  and second order accurate in  $(\Delta r)$ . An artificial viscosity parameter ( $\varepsilon$ ) is added to make it second order in  $(\Delta\theta)$ . However, reducing  $(\Delta\theta)$  may lead to oscillatory behaviour particularly in regions of the flow where strong shock wave(s) may occur and a large value of ( $\varepsilon$ ) is used. Default values for ( $\varepsilon$ ) are shown in table 1.
- III. In the backward differencing scheme, oscillatory behaviour may also occur due to the mapping procedure specifically if a large reduction in profile (aerofoil) first derivative occurs downstream of the maximum suction point (lowest pressure point on the upper surface of the aerofoil).

B. Stability

- I. The central differencing scheme is unconditionally stable. However, any oscillatory behaviour in fully subsonic flow will only be due to the profile input data (if not a smooth function) and the resulting cubic spline used in the conformal mapping procedure.
- II. The backward differencing scheme is conditionally stable based on equation (10) and the situations described therein.

C. Convergence

- I. The central difference scheme is unconditionally convergent.
- II. For the backward differencing scheme, relaxation factors are used to speed up the iterative process and help conversion. These are stipulated in equation (18, 19) and figure (5).

## 6. Recommendations

Based on the results of this study it is recommended that:

- A. The VGK method can be used and will provide reliable data (very close to experimental results) over profiles defined by smooth functions up to free stream speeds and angles of attack that will not cause the flow to reach a critical Mach number (fully subsonic flow).
- B. For flows where local weak shock waves ( $M_{shock} < 1.4$ ) VGK can still be used but a careful examination of the iterative procedure must be considered. (an output file of VGK with an (.IEH) extension facilitates this check)
- D. For difficult flows (strong shock waves) and/or non-smooth profiles (for example aerofoils with indentations), the grid resolution effects  $(\Delta\theta, \Delta r)$  on the consistency, stability and convergence of the VGK must be investigated further. The present author modified the code by increasing the grid resolution to (360) radial lines instead of the original maximum (160) lines. The present author intends to investigate the effects of this modification on the VGK performance. The results of the intended study will be in a separate future paper.

## References

- [1]. Freestone, M.M. "ESDU Transonic Aerodynamics Vol.3, 1997"
- [2]. Jameson,A. "Full potential,Euler and Navier-Stokes Schemes",chapter 3 in "Applied computational aerodynamics",progress in aeronautics and astronautics,Henne,P.A, Editor,Vol.125,1990
- [3]. Anderson, J.D. "Computational fluid dynamics, the basics with applications". McGraw Hill Int., 1996.
- [4]. Hutchison M J. "Investigation into the ability of two CFD codes to model aerodynamic effects of airframe surface imperfections", ESDU Paper 365,ESDU. July 1994.
- [5]. Salah.J.S EL-IBRAHIM. "Prediction of the effects of aerofoil surface irregularities at high subsonic speeds using the viscous Garabedian & Korn method". PhD thesis. Department of Civil Aeronautical and Mechanical Engineering, University of Hertfordshire, U.K., unpublished work,2000.
- [6]. Freestone, M.M. "VGK Method for two-dimensional aerofoil sections- part1: Principles and results". Draft Data Item, ESDU international, Oct.1996.
- [7]. Hirsch C. "Numerical computation of internal and external flows". Volume 1, "Fundamentals of numerical discretization". Wiley series in numerical methods in engineering ,John Wiley & Sons. 1989.
- [8]. Hirsch C. "Numerical computation of internal and external flows". Volume 2, "Computational methods for inviscid and viscous flows". Wiley series in numerical methods in engineering ,John Wiley & Sons. 1990.
- [9]. Hoffman J.D. "Numerical methods for engineers and scientists". McGraw-Hill International editions.1993.
- [10]. Murman, E.M. Cole, J.D. "Calculation of plane steady flows". AIAA Journal.Vol.9, No.1. January 1971.
- [11]. Fletcher C.A. "Computational techniques for fluid dynamics, Volume I, -Fundamentals and general techniques". Springer-Verlag ,2nd edition,1991.
- [12]. Collyer, M.R. "An extension to the method of Garabedian & Korn for the calculation of transonic flow past an aerofoil to include the effects of a boundary layer and wake". Reports &Memoranda No.3828.RAE, July 1977.
- [13]. Lock, R. C. , Collyer,M.R " A modification to the method of Garabedian & Korn". Numerical methods for the calculation of inviscid transonic flows. FREDR VIEWE GUND S. 1981